Available online at www.sciencedirect.com

SciVerse ScienceDirect

Proceedings of the Combustion Institute 34 (2013) 865–872

Proceedings of the Combustion Institute

www.elsevier.com/locate/proci

Flame acceleration in long narrow open channels

Vadim N. Kurdyumov [a,*], Moshe Matalon [b]

[a] Department of Energy, CIEMAT, Avda. Complutense 40, Madrid, Spain
[b] Mechanical Science and Engineering, University of Illinois at Urbana-Champaign, Urbana, IL 61801, USA

Available online 11 August 2012

Abstract

We study the propagation of premixed flames in long but finite channels, when the mixture is ignited at one end and both ends remain open and exposed to atmospheric pressure. Thermal expansion produces a continuous flow of burned gas directed away from the flame and towards the end of the channel where ignition took place. Owing to viscous drag, the flow is retarded at the walls and accelerated in the center, producing a pressure gradient that pushes the unburned gas ahead of the flame towards the other end of the channel. As a result the flame accelerates when it travels from end to end of the channel. The total travel time depends on the length of the channel and is proportional to $\gamma^{-1}\ln(1+\gamma)$, where γ is the heat release parameter.

Keywords: Premixed flames; Flame acceleration; Flame propagation in tubes

1. Introduction

The problem of flame propagation in long tubes has attracted interest since the early flame studies of Mallard and Le Chatelier [1]. A combustible mixture contained in a tube is ignited at one end and the subsequent motion of the flame is followed. The problem is of great interest in safety applications, and it is a precursor for the transition from deflagration to detonation. Moreover, such a configuration has been often used for measurements of the laminar burning velocity.

It has been recognized in the early studies of Mason and Wheeler [2] and Guénoche [3] that the geometry of the tube and the boundary conditions that it imposes are parameters that affect the flame propagation. Unlike freely propagating flames, when restricted by walls the flow induced by thermal expansion affects the expansion of the burned gas and consequently the velocity of the unburned gas and the propagation of the flame. Different flame behaviors were observed when one or both ends of the tube remain closed, or if both ends were held open. This study is concerned with flame acceleration, observed when the mixture is ignited at one end and both ends remain open.

Intrigued by the observation that flames in channels are always convex towards the unburned gas, the early theoretical studies of flames in tubes and channels were concerned with the flame structure and stability. Several studies have focused on explaining the observed shape [4], the effects of tube diameter [5] and stability aspects of the curved structure [6]. We now understand that because of the hydrodynamic instability that results from thermal expansion [7,8] flat flame cannot be realized except in sufficiently narrow channels where diffusion exerts stabilizing influences [9,10].

* Corresponding author.
E-mail address: vadim.k@ciemat.es (V.N. Kurdyumov).

1540-7489/$ - see front matter © 2012 Published by Elsevier Inc. on behalf of The Combustion Institute.
http://dx.doi.org/10.1016/j.proci.2012.07.045

Recent studies conducted within the framework of a constant density approximation have examined the flame response to imposed hydrodynamic conditions, without accounting for the effect of the flame on the flow that results from thermal expansion. Despite the simplification adopted, various phenomena were captured including the flame response to a Poiseuille flow assisting or opposing the flame [11], the effects of thermally active walls [12] and of heat losses [13], and the influence of differential diffusion [14–16]. Numerical studies that properly account for thermal expansion have re-examined these issues and extended the research scope to examine various modes of flame propagation, including asymmetric and oscillatory flames [17–19], as well as aspects of flame dynamics in narrow-to-moderate channels [20]. The problem of a flame propagating in a tube or channel open at both ends, which is the focus of the present work, has not been studied before.

Starting from the general conservation laws we first derive equations applicable to narrow channels. We then address the resulting problem, analytically using a quasi-steady approximation and numerically by solving the time-dependent problem with initial conditions that simulate an ignition event. For simplicity, associated mainly with the numerical calculations, we consider here the two-dimensional case and comment on the minor modifications that result in the formulation of the equivalent problem of flame propagation in narrow circular tubes. Results and conclusions are presented in the last sections.

2. Formulation

We consider a channel of length L and width h, with adiabatic walls. For definiteness, we assume that the mixture is ignited at the left end, i.e., at $x = 0$. Upon ignition, the diaphragms containing the mixture in the channel are simultaneously removed, and both ends of the channel remain open and exposed to atmospheric pressure. Of interest is to examine the propagation in sufficiently long channels, but of finite length.

The combustible mixture undergoes a chemical reaction modeled by a global irreversible step $F + O \rightarrow P$, where F denotes the fuel, O the oxidizer and P the products. The fuel consumed per unit volume, per time, is given by

$$\omega'_F \sim \left(\frac{\rho' Y_F}{W_F}\right)\left(\frac{\rho' Y_O}{W_O}\right)\exp(-E/\mathcal{R}T'),$$

where Y_F, Y_O are the mass fractions and W_F, W_O the molecular weights of the fuel and oxidizer, respectively, ρ' is the density of the mixture, E is the overall activation energy, $\mathcal{R}$ is the universal gas constant and T' is the temperature (primes here and thereafter denote dimensional quantities). Assuming the mixture is lean in fuel, the oxidizer mass fraction remains nearly constant and $\omega'_F = \mathcal{B}\rho'^2 Y_F \exp(-E/\mathcal{R}T')$, where $\mathcal{B}$ is a pre-exponential factor containing Y_O.

Let x', y' be, respectively, the longitudinal and transverse coordinates (Fig. 1) with u', v' the corresponding velocity components. If the speed S_L and thermal thickness δ_T of a planar adiabatic flame are used as reference, and the ratio of the channel width to the flame thickness is denoted by $a \equiv h/\delta_T$, appropriate dimensionless variables are $x = x'/\delta_T$, $y = y'/h$, $t = S_L t'/\delta_T$, $u = u'/S_L$, $v = v'/aS_L$. We also introduce $\rho = \rho'/\rho_u, p = a^2 p'/\rho_u S_L^2$, $\theta = (T' - T_u)/(T_a - T_u)$, $Y = Y'/Y_{F_u}$- as dimensionless values for the density, pressure and temperature, where ρ_u, T_u $Y_{F_u}$are the values of density, temperature and fuel mass fraction in the fresh mixture. Here p' is the pressure deviation from the ambient (atmospheric) pressure P_0 which, in view of the low Mach number approximation adopted here, is constant, and $T_a = T_u +$ $QY_{F_u} c_p$ is the adiabatic flame temperature where Q is the total heat release and c_p the specific heat (at constant pressure) of the mixture. The thermal thickness of the flame is given by $\delta_T = \mathcal{D}_T/S_L$, where $\mathcal{D}_T$ is the thermal diffusivity of the mixture.

The nondimensional equations, describing conservation of mass, momentum and energy take the form

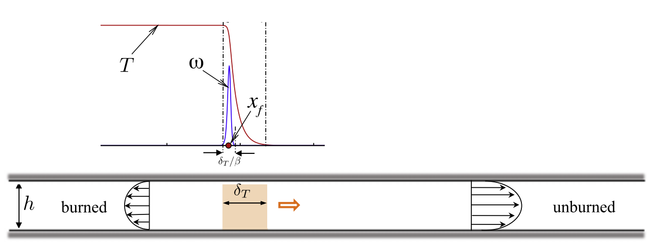

Fig. 1. Sketch of the channel configuration, illustrating the various length scales associated with the flame propagation problem.

$$\rho_t + (\rho\, u)_x + (\rho\, v)_y = 0, \qquad (1)$$

$$\rho(u_t + uu_x + vu_y) = a^{-2}(-p_x + \Pr\, u_{yy}) + \Pr\left[\frac{4}{3}u_{xx} + \frac{1}{3}u_{xy}\right], \qquad (2)$$

$$\rho(v_t + uv_x + vv_y) = -a^{-4}p_y + \Pr\left[a^{-2}\left(\frac{4}{3}v_{yy} + \frac{1}{3}u_{xy}\right) + v_{xx}\right], \qquad (3)$$

$$\rho(\theta_t + u\theta_x + v\theta_x) - (\theta_{xx} + a^{-2}\theta_{yy}) = \omega, \qquad (4)$$

$$\rho(Y_t + uY_x + vY_y) - Le^{-1}(Y_{xx} + a^{-2}Y_{yy}) = -\omega, \qquad (5)$$

where $\rho = 1/(1+\gamma\theta)$is the equation of state, with $\gamma = (T_a - T_u)/T_u$ the heat release parameter. The Prandtl number, $Pr = \nu/\mathcal{D}_T$, representing the ratio of the viscous to thermal diffusivities of the mixture, and the Lewis number, $Le = \mathcal{D}_T/\mathcal{D}_F$, representing the ratio of the thermal diffusivity of the mixture to the mass diffusivity of the fuel, were taken as constants.

In writing the dimensionless expression for the reaction rate ω, it is convenient to introduce the asymptotic expression for the laminar flame speed

$$(S_L)_{\text{asp}} = \sqrt{2Le\mathcal{B}\rho_u\mathcal{D}_T/\beta^2}\,(\rho_b/\rho_u)\,\mathrm{e}^{-E/2\mathcal{R}T_a},$$

derived for $\beta \gg 1$, where $\beta = E(T_a - T_u)/\mathcal{R}T_a^2$ is the Zel'dovich number and $\rho_b = \rho_u T_u/T_a$ is the density of the burned gas. Then

$$\omega(\theta, Y) = \frac{\beta^2}{2s_L^2 Le}\left(\frac{1+\gamma}{1+\gamma\theta}\right)^2 Y \times \exp\left\{\frac{\beta(\theta-1)}{(1+\gamma\theta)/(\gamma+1)}\right\}, \qquad (6)$$

where $s_L = S_L/(S_L)_{\text{asp}}$. For a finite value of the Zel'dovich number β and given γ and Le the laminar flame speed, or equivalently the factor s_L, must be determined numerically as the eigenvalue of the following boundary-value problem

$$-\theta^I = \theta^{II} + \omega, \quad -Y^I = Le^{-1}Y^{II} - \omega,$$
$$x \to \infty : \theta = Y - 1 = 0; \quad x \to -\infty : \theta^I = Y^I = 0, \qquad (7)$$

where ω is given by (6). This problem describes the structure of a planar adiabatic flame propagating along the positive x-axis at a constant speed S_L, and can be easily solved numerically. Clearly, the factor s_L tends to one when $\beta \to \infty$. For finite β the asymptotic formula over- or under-estimate the value of S_L depending on the Lewis number Le; the values of s_L for $\beta = 10$ and $Le = 1$ are 1.0652, 1.0588 and 1.0548 for $\gamma = 3$, 4 and 5, respectively.

At the channel walls we assume no-slip and adiabatic conditions, so that

$$u = v = 0, \quad \partial\theta/\partial y = \partial Y/\partial y = 0, \quad \text{at } y = 0, 1. \qquad (8)$$

While premixed flames generally quench when the channel width is below the quenching distance, for adiabatic walls a flame will always propagate through. It is also assumed, for simplicity, that conditions at both ends remain adiabatic so that

$$\partial\theta/\partial x = \partial Y/\partial x = 0, \quad \text{at } x = 0, \ell, \qquad (9)$$

where $\ell = L/\delta_T$ is the channel length measured in units of the flame thickness. The temperature and mass-fraction conditions (9) represent the typical outlet boundary conditions applied for cases where the flow velocity is directed outside the end of the channel. Modifications are required when the flame is near the ends, more specifically within a distance $O(a)$ from the ends. Nevertheless, these instants are small in sufficiently long channels compared with the entire propagation time and considered negligible in the present study.

Since following ignition the channel remains open, the pressure at both ends is constant and equal to the ambient pressure, so that

$$p = 0 \quad \text{at } x = 0, \ell. \qquad (10)$$

These conditions require some clarification, because the pressure at the immediate exit of the channel is determined, in general, by the flow divergence and is therefore a function of the representative Reynolds number Re. Navier–Stokes calculations inside and outside the channel show that for finite but moderate Re the pressure drop continues slightly beyond the tube exit and attains a minimum before reaching the ambient pressure. In long narrow tubes the pressure drop is very small and extends only a short distance comparable to the tube radius, which justifies our assertion of imposing the condition (10) immediately at $x = 0$ and $x = \ell$.

3. Narrow channels

We consider now the case of a narrow channel, $a \ll 1$, corresponding to a channel height much smaller that the flame thickness. The asymptotic treatment follows that presented in [11,13]. Accordingly, all variables are expanded in power series of a^2, namely in the form $f = f_0 + a^2 f_1 + \cdots$, where f stands for the temperature θ, the mass fraction Y, the pressure p and the velocity components u and v.

To leading order $\partial^2 Y_0/\partial y^2 = 0$, $\partial^2\theta_0/\partial y^2 = 0$ which, when integrated with respect to y and using the boundary conditions (8), implies that $Y_0 = Y_0(x,t)$, $\theta_0 = \theta_0(x,t)$ and $\rho_0 = \rho_0(x,t)$. The equation of state implies that $\rho_0 = (1+\gamma\theta_0)^{-1}$.

The momentum equations, to leading order, yield

$$\partial p_0/\partial y = 0, \quad \partial p_0/\partial x = \Pr\, \partial^2 u_0/\partial y^2. \qquad (11)$$

The first implies $p_0 = p_0(x,t)$, and permits a direct integration of the second equation. Using the boundary conditions (8) one finds

$$u_0 = 6U\,y(1-y), \tag{12}$$

where U is the mean axial velocity across the channel, given by

$$U(x,t) = \int_0^1 u_0\,dy = -\frac{1}{12\mathrm{Pr}}\left(\frac{\partial p_0}{\partial x}\right). \tag{13}$$

The continuity equation can now be integrated to give

$$\rho_0 v_0 = -\left[\frac{\partial \rho_0}{\partial t}y + \frac{\partial(\rho_0 U)}{\partial x}(3y^2 - 2y^3)\right],$$

where $v_0 = 0$ at $y = 0$ has been satisfied. The second boundary condition, $v_0 = 0$ at $y = 1$, implies

$$\frac{\partial \rho_0}{\partial t} + \frac{\partial(\rho_0 U)}{\partial x} = 0. \tag{14}$$

Hence, the transverse velocity

$$v_0 = \frac{1}{\rho_0}\frac{\partial(\rho_0 U)}{\partial x}y(2y^2 - 3y + 1). \tag{15}$$

Integrating Eq. (13) from one end of the channel to the other and imposing the conditions (10) yields the following constraint on the mean flow rate

$$\int_0^{\ell} U(x,t)\,dx = 0. \tag{16}$$

At this stage the temperature θ_0 and mass fraction Y_0 remained undetermined, which require considering the governing equations (4) and (5) to the next order. These reduce to

$$\frac{\partial^2\theta_1}{\partial y^2} = \rho_0\frac{\partial\theta_0}{\partial t} + \rho_0 U\frac{\partial\theta_0}{\partial x} - \frac{\partial^2\theta_0}{\partial x^2} - \omega(\theta_0, Y_0),$$

$$\frac{1}{Le}\frac{\partial^2 Y_1}{\partial y^2} = \rho_0\frac{\partial Y_0}{\partial t} + \rho_0 U\frac{\partial Y_0}{\partial x} - \frac{1}{Le}\frac{\partial^2 Y_0}{\partial x^2} + \omega(\theta_0, Y_0).$$

Integrating across the channel and using the boundary conditions (8), the left hand side of each of these two equations vanishes resulting in equations for θ_0 and Y_0 as solvability conditions. Dropping the subscript "0" for simplicity of notation, the problem to leading order reduces to

$$\rho\theta_t + \rho U\theta_x - \theta_{xx} = \omega, \tag{17}$$

$$\rho Y_t + \rho U Y_x - Le^{-1}Y_{xx} = -\omega, \tag{18}$$

where $\rho = (1+\gamma\theta)^{-1}$, to be solved together with (14) subject to the constraint (16).

Hence, in narrow channels the flame remains nearly planar but is subjected to a mean flow that varies in time and is constrained by friction forces at the walls or, equivalently, by the pressure conditions at the two ends. In the following we first examine the problem by adopting a quasi-steady approximation valid for long channels and then address the time-dependent problem numerically for finite values of ℓ. It should be noted that Eqs. (14) and (17,18) equally applies to flame propagation in narrow circular tubes, when the mean velocity U is properly defined. The expressions (12)–(15) for u_0 and v_0 are slightly modified to accommodate for the circular geometry, but the constraint (16), and hence the results of the quasi-steady approximation presented next, remain valid.

4. Quasi-steady approximation

The propagation of the flame is characterized by the time δ_T/S_L required for the flame to travel a distance comparable to the flame thickness. In long channels ($\ell \gg 1$), this time is much shorter that the time required for the flame to propagate throughout the entire channel $L/S_L = \ell(\delta_T/S_L)$ and affected by the slow variations in the mean flow rate U. The flame may then be treated as propagating quasi-steadily, an assumption that remains valid throughout the entire time except for two short instances. The first corresponds to the short time interval during which the flame separates from the ignition end, and the second the time interval when the flame is sufficiently close to the far end of the channel.

It is convenient to introduce a coordinate $\xi = x - x_f(t)$ attached to the *flame front*, defined as the position $x_f(t)$ where the reaction rate ω reaches its maximum value. Then $\partial/\partial t \to -\dot{x}_f\,\partial/\partial\xi$ where the "dot" corresponds to differentiation with respect to t. Equations (14)–(18) reduce to

$$\frac{\partial}{\partial\xi}[\rho(U - \dot{x}_f)] = 0, \tag{19}$$

$$[\rho(U - \dot{x}_f)]\frac{\partial\theta}{\partial\xi} - \frac{\partial^2\theta}{\partial\xi^2} = \omega, \tag{20}$$

$$[\rho(U - \dot{x}_f)]\frac{\partial Y}{\partial\xi} - \frac{1}{Le}\frac{\partial^2 Y}{\partial\xi^2} = -\omega. \tag{21}$$

Equation (19) implies that $\rho(U - \dot{x}_f) = C$, with $C = -1$ obtained by direct comparison with (7). The mean flow velocity in the channel is thus given by

$$U = \dot{x}_f - (1 + \gamma\theta). \tag{22}$$

Analytical solution of Eqs. (20) and (21) can be obtained in the asymptotic limit $\beta \to \infty$ and the reaction zone is then confined to a region of thickness β^{-1} near $\xi = 0$. With the exception of short instants when the flame is near the ends of the channel, the solution outside of the reaction zone becomes

$$\theta = \begin{cases} 1 \\ e^{-\xi} \end{cases}, \quad Y = \begin{cases} 0 & \xi < 0 \\ 1 - e^{-Le\,\xi} & \xi > 0 \end{cases},$$

where the exponentially small terms were neglected. The discontinuity in slopes at $\xi = 0$ is smoothed-out in the thin reaction zone. Substituting into (16) one obtains

$$\dot{x}_f - \frac{\gamma}{\ell}x_f = 1 + \frac{\gamma}{\ell} - \frac{\gamma}{\ell}\, e^{x_f - \ell}. \tag{23}$$

For large ℓ, the last term is exponentially small and may be neglected. The resulting equation can be solved subject to the initial condition $x_f(0) = 0$ to provide an expression for the history of the flame position

$$x_f = \left(\frac{\ell}{\gamma} + 1\right)\left[\exp\left(\frac{\gamma t}{\ell}\right) - 1\right]. \tag{24}$$

When $\gamma \to 0$, this relation reduces to $x_f = t$ implying that the flame propagates steadily at a constant speed. In long but finite channels and when the heat release is substantial, the flame accelerates through the channel. The total time required for the flame to travel the entire channel is

$$t_{\text{tot}} = \frac{\ell}{\gamma}\ln\left(1 + \frac{\gamma\ell}{\ell + \gamma}\right) \approx \frac{\ell}{\gamma}\ln(1 + \gamma). \tag{25}$$

Note that the results (24) and (25) are independent of the Lewis number Le. The dimensional counterpart, however, depends on Le through δ_T or S_L. This result is consistent with the conclusions drawn in [21] where it was shown that variations in Lewis number have a pronounced effect on *thin flames*, or flames in relatively wider channels, but has practically no effect on *thick flames*, or flame in narrow channels.

We note parenthetically that the position of a flame propagating from a closed end, or towards a closed end of a channel, can be easily deduced from Eq. (22). When the flame propagates from the closed ignition end, the volume expansion rate is proportional to the distance traveled. In this case $U = 0$ at $x = 0$, which together with the condition $\theta = 1$ implies that $\dot{x}_f = 1 + \gamma$. When the flame propagates to the closed end, there is no gas motion far ahead of the flame. Then $U = 0$ at $x = \ell$, while $\theta = 0$ there, implying that $\dot{x}_f = 1$. In both cases the flame propagates steadily throughout the channel.

Considering $\ell \gg 1$ in Eq. (24) shows that early in the development of flame propagation, as long as $1 \ll t \ll t_{\text{tot}}$, the flame motion is similar to the propagation to the closed end, namely $\dot{x}_f \approx 1$. Nevertheless at a considerable distance from the ignition end, as $t \sim t_{\text{tot}}$, the finite length of the channel has its impact being intrinsically included in the propagation velocity.

5. Numerical methodology

The numerical solution of the time-dependent equations (14) and (17)–(18) was obtained using an explicit time marching procedure. Because of the presence of the highly nonlinear reaction rate term, a sufficiently small time step Δt was found necessary in order to ensure numerical stability; typically $\Delta t \approx 10^{-5}$ was used in the calculations. Spatial derivatives were discretized using a second-order, three-point central difference scheme on the uniform grid with a resolution of $\Delta x = 0.05$. In some cases the number of grid points was doubled to test the independence of the solution to the selected grid. The independence of the solution to the selected time step was verified by comparing time histories of $x_f(t)$ calculated with different Δt.

The following observation was found useful and facilitated the computations. By adding Eqs. (14) and (17) after multiplying the latter by γ, and using $\rho(1 + \gamma\theta) = 1$ one finds that $\partial U/\partial x = \gamma(\partial^2\theta/\partial x^2 + \omega)$. Integrating with respect to x and using the constraint (16) to determine the constant of integration (which here depends on t), yields

$$U(x,t) = \widetilde{U}(x,t) - \frac{1}{\ell}\int_0^\ell \widetilde{U}(x,t)dx, \tag{26}$$

where

$$\widetilde{U}(x,t) = \gamma\int_0^x \left(\frac{\partial^2\theta}{\partial x^2} + \omega\right)dx.$$

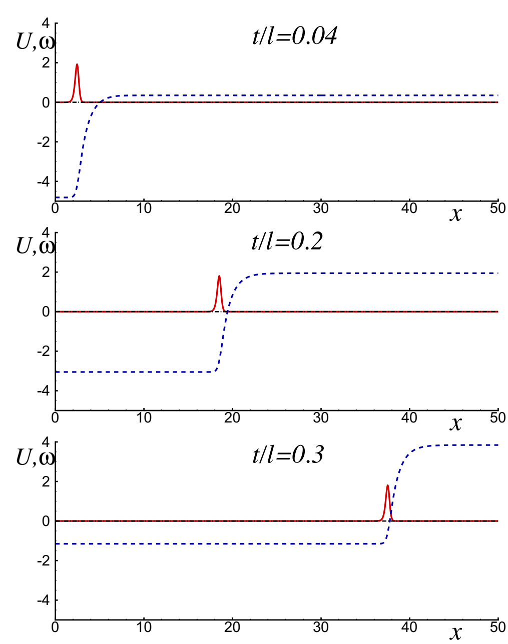

Fig. 2. The mean flow rate U along the channel (shown as a dashed curve) at different times, calculated for a channel of length $\ell = 50$; the reaction rate ω represented by a solid curve marks the location of the reaction zone.

At each time step the mean flow velocity $U(x,t)$ may therefore be calculated from (26), and one only need to integrate Eqs. (17) and (18).

The initial conditions imposed were in the form of a hot spot located near the left end of the channel. Specifically, θ was specified to be larger than zero in a small region close to the end and Y was assumed to be uniformly distributed throughout the entire channel. In all cases, it was verified that $x_f(t)$, after a short transient sufficiently smaller that $t_{\rm tot}$, becomes independent on the specified initial conditions. For the smaller

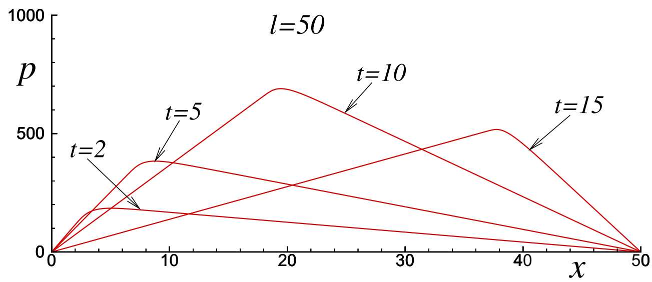

Fig. 3. The pressure distribution along the channel at different times, calculated for a channel of length $\ell = 50$.

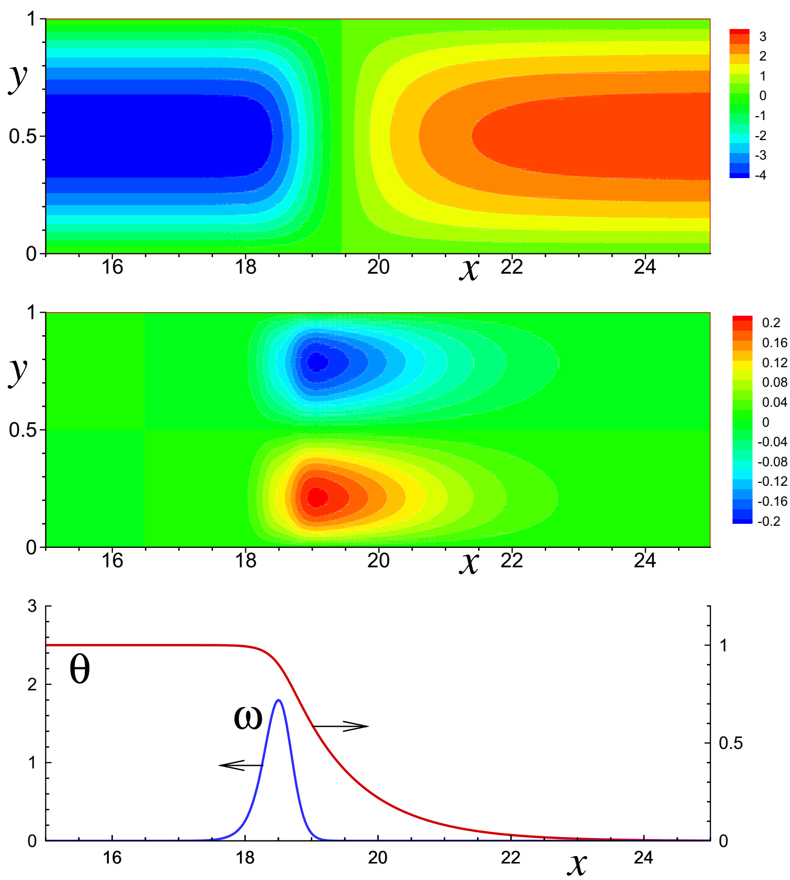

Fig. 4. The flow field in the vicinity of the flame; the two color figures show the axial/transverse velocity distribution in the channel.

value of $\ell = 50$ considered, variations in $x_f(t)$ due to different initial conditions were found to be within 0.1%.

The numerical results presented below were carried out for $\beta = 10$, which is a representative value for hydrocarbon flames.

6. Results

Figure 2 shows the variations of the mean axial velocity U along the channel for several values of t. The reaction rate ω is plotted on the same figure to mark the instantaneous position of the reaction zone. Immediately upon ignition a premixed flame propagates to the right, and a flow of burned gases is produced as a result of thermal expansion moving towards the end of the channel where ignition took place. As a result of viscous drag the flow is retarded at the walls and accelerates in the center of the channel, creating a thrust that pushes the unburned gas towards the other end of the channel. Figure 3 shows the pressure distribution along the channel at various times that support this description. The two-dimensional flow field in the vicinity of the flame, as described by (12) and (15), is shown in Fig. 4. Elsewhere, U is practically constant but has opposing signs, which implies that $v \approx 0$ and Poiseuille flows develop moving to the left or to the right.

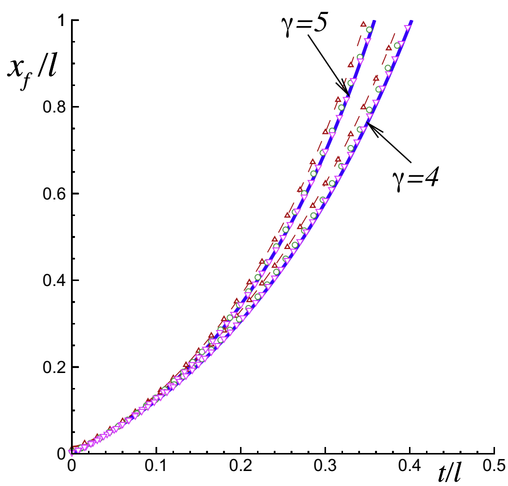

Fig. 5. History of flame position x_f, for different values of γ. The symbols $\triangle$, $\circ$, ∇ correspond to $\ell = 50$, 100, 500, respectively, and the solid curve corresponds to the quasi-steady analytical approximation.

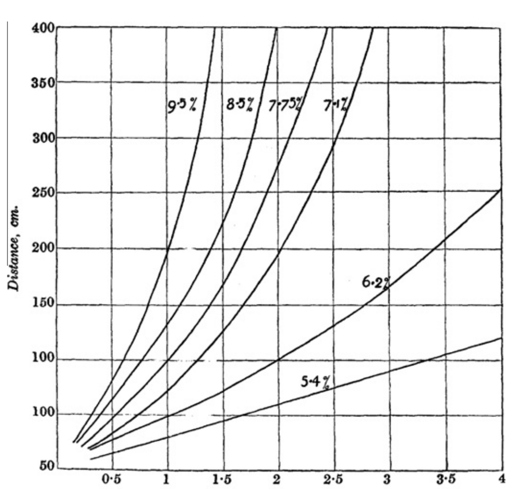

Fig. 6. Position of a methane–air flame propagating in a long tube open at both ends for different mixture strength; reproduced from [2].

Figure 5 shows the time history of the flame position x_f in channels of length $\ell = 50$, 100, 500 (distinguished by different symbols) for two distinct values of γ. The analytical quasi-steady approximation (24) is shown as a solid curve. The ordinate x_f/ℓ is the (dimensional) flame position in units of the channel length L, and the abscissa t/ℓ is the (dimensional) time in units of S_L/L. Using these scales we see that for a given γ the curve representing the flame position as a function of time become universal for large ℓ. Furthermore, the quasi-steady approximation represents the time-dependent solution extremely well in this limit, implying that the approximate (dimensional) relation

$$x'_f = \left(\frac{L}{\gamma}\right)\left[\exp\left(\frac{\gamma S_L t'}{L}\right) - 1\right] \tag{27}$$

is sufficient accurate. The total travel time in long tubes ($L \gg \delta_T$) is given by

$$t'_{\rm tot} \approx \frac{\ln(1+\gamma)}{\gamma}\,\frac{L}{S_L}. \tag{28}$$

Note that these relations are independent of the Lewis number Le and the activation energy β, except for their effect on S_L. Thus, for flames propagating in narrow channels, chemistry and differential diffusion manifest themselves solely through variations in the laminar flame speed S_L.

The experimental results of Mason and Wheeler [2] reproduced in Fig. 6 show the flame position of methane–air mixtures ignited at one end of a tube open at both ends. Although the experiments were carried out in a relatively wide tube, 5 cm in diameter, the observations clearly show the acceleration of the flame traveling down the tube. The different curves in the figure correspond to increasing values of the mixture strength and, since the parameter that mostly affect the equivalence ratio is the heat release, they also correspond to increasing values of γ and thus show a similar trend as our predictions depicted in Fig. 5.

The total propagation time in the 500 cm-long tube estimated from the experimental results is within the range $2-5.5$ s, which compares surprising well with the predicted value of 4.3 s obtained from (28) with $\gamma = 6.36$ and $S_L = 36.2$ cm/s, as appropriate for methane–air mixtures.

7. Conclusions

The objective of this study has been to examine the nature of flame propagation in long tubes open at both ends and, in particular, the physical mechanism causing the flame to accelerate as it travels down the tube. The mathematical problem involves, in general, solving the unsteady two-dimensional equations governing mass, momentum and energy, which must be carried out for a whole range of parameters, including the length and aspect ratio of the tube and the mixture properties, which is clearly a nontrivial task. In this work, the narrow channel assumption was adopted in order to simplify the mathematical problem and gain fundamental understanding that would have otherwise require lengthy numerical simulations. Such calculations are seldom done for an entire range of parameters and are usually carried out for a specified set of parameter values. Moreover, the adopted simplifications in this work enabled extracting simple results such as Eqs. (26) and (27) for the flame position and total travel time, and graphs such as Fig. 5 where these expressions were further validated. It is also well known that asymptotic methods provide approximations that could very well extend beyond their strict limit of validity. It is very unlikely that the flow field will change dramatically from a Poiseuille flow unless the channel is sufficiently wide and that the flame will no longer accelerate if it were slightly curved. The evidence that the approximation adopted is useful is that it produces results that agree qualitatively, and to some extent also quantitatively, with the experimental results reported in Fig. 6 even though the channel width in these experiments was quite moderate. Finally, we note that we have addressed here flame propagation in sufficiently long channels, where the flame is remote and not affected by the two ends; the modifications required when the flame is near the ignition end ($x = 0$) and near the end of the tube ($x = \ell$), do not affect the main result associated with the acceleration observed during "almost" the entire propagation time.

Acknowledgments

M.M. acknowledges partial support by the National Science Foundation under Grant CBET-1067259. V.K. acknowledges the support of Spanish MEC under projects #ENE2011-27686-C02-01 and CSD2011-00011.

References

[1] E. Mallard, H.L. Le Chatelier, *Ann. Mines* 4 (1883) 274–388.
[2] W. Mason, R.V. Wheeler, *J. Chem. Soc. Trans.* 117 (1920) 36–47.
[3] H. Guénoche, in: G. Markstein (Ed.), *Unsteady Flame Propagation*, Macmillan, 1964, pp. 107–181 (Chapter E).
[4] M.S. Uberoi, *Phys. Fluids* 2 (1959) 1–7.
[5] T. Maxworthy, *Phys. Fluids* 5 (4) (1962) 407–417.
[6] Y.B. Zel'dovich, A.G. Istratov, N.I. Kidin, V.B. Librovich, *Combust. Sci. Technol.* 24 (1980) 1–13.
[7] G. Darrieus, Propagation d'un front de flamme, Unpublished work, 1938.
[8] L.D. Landau, *Acta Physicochim. USSR* 19 (1944) 77–85.
[9] G.I. Sivashinsky, *Proc. Combust. Inst.* 29 (2002) 1737–1761.
[10] M. Matalon, *Proc. Combust. Inst.* 32 (2009) 57–82.
[11] J. Daou, M. Matalon, *Combust. Flame* 124 (2001) 337–349.
[12] D.A. Kessler, M. Short, *Combust. Theory Model.* 12 (5) (2008) 809–829.
[13] J. Daou, M. Matalon, *Combust. Flame* 128 (2002) 321–339.
[14] V.N. Kurdyumov, E. Fernández-Tarrazo, *Combust. Flame* 128 (2002) 382–394.
[15] C. Cui, M. Matalon, T.L. Jackson, *AIAA J.* 43 (6) (2005) 1284–1292.
[16] V.N. Kurdyumov, *Combust. Flame* 158 (2011) 1307–1317.
[17] P. Metzener, M. Matalon, *Combust. Theory Model.* 5 (2001) 463–483.
[18] D.G. Norton, D.G. Vlachos, *Chem. Eng. Sci.* 58 (2003) 4871–4882.
[19] C. Tsai, *Combust. Sci. Technol.* 18 (2008) 533–545.
[20] M. Short, D.A. Kessler, *J. Fluid Mech.* 638 (2009) 305–337.
[21] C. Cui, M. Matalon, J. Daou, J. Dold, *Combust. Theory Model.* 8 (2004) 41–64.